

SOME EFFECTS OF METALLIC SUBSTRATE COMPOSITION ON DEGRADATION OF THERMAL BARRIER COATINGS

I. G. Wright, B. A. Pint, W. Y. Lee*, K. B. Alexander, and K. Prübner
Oak Ridge National Laboratory, Oak Ridge, Tennessee, USA.

ABSTRACT

Comparisons have been made in a laboratory cyclic oxidation test of the modes of degradation of single crystal superalloy substrates and bond coating alloys intended for use with thermal barrier coatings systems. The influence of desulphurisation of the superalloy and bond coating, of reactive element addition to the bond coating alloy, and of oxidation temperature on the spallation behavior of the alumina scales formed was assessed from oxidation kinetics and from observations of the structure and composition of the metal-oxide interfaces. Desulphurisation of a nickel-base superalloy (in the absence of a Y addition) resulted in an increase in the lifetime of a state-of-the-art thermal barrier coating applied to it. The lifetime of the same ceramic coating applied to a model bond coating alloy (doped with a reactive element but not desulphurised) that formed an 'ideal' alumina scale was found to be, in the same test, at least four times longer than on the Y-doped superalloy plus state-of-the-art bond coating combination. Some explanations are offered of the factors controlling the degradation of such coatings.

BACKGROUND

As part of the Materials and Manufacturing segment of the U. S. Department of Energy's Advanced Turbine System (ATS) program [1], efforts are being made to facilitate the scale-up of single crystal casting processes for industrial turbine-sized vanes and blades [2,3], and to develop improved thermal barrier coating systems for these components [4,5]. An integral part of the casting program is the development of a production-scale process for desulphurising the alloys to avoid the need for small alloying additions of yttrium, the levels of which are difficult to control in the single crystal casting process without using alumina cores and face coats on the molds.

Studies by several groups, including Ikeda [6], Funkenbusch, Smeggil and Bornstein [7-9], Luthra [10], Smialek, et al. [11-16], Schaeffer et al., [17], and Meier, et al. [18], have shown that lowering the tramp sulphur content of alumina scale-forming alloys to sub-ppm (atomic) levels can dramatically improve the resistance to scale loss by spallation. For those studies, the desulphurisation was typically achieved by hydrogen annealing of relatively thin specimens at temperatures of 1200°C or greater, under conditions where the alloy surface remained scale-free so that any sulphur diffusing to that surface could react with hydrogen and be removed. Smialek [13] suggested that, for optimum improvement in resistance to spallation, the total sulphur content of a component should be reduced to less than the level required to produce one monolayer upon segregation; for specimens of the thickness used in this study, this corresponded to approximately 0.4 ppm [14,16].

Comparisons of the influence of sulphur and reactive element additions led to the suggestion that the role of reactive elements such as yttrium is to prevent sulphur segregation during oxidation [7]. Identification of yttrium sulfides in the alloy substrate [19] was used to justify an argument for sulphur gettering by yttrium, whereas others have proposed that the role of yttrium is to modify the surface energy of the relevant interfaces, thereby inhibiting the segregation of sulphur to those locations [20]. Other observations suggest that reactive element additions exert the further effect of slowing the rate of growth of alumina scales as a result of incorporation of the reactive element ions into the oxide, and their segregation to the oxide grain boundaries [20-22].

The focus of the study reported here is on routes to developing a practically 'ideal' protective alumina scale on alloys used as bond coatings on nickel-base superalloys, as a contribution to maximising the life of the thermal barrier coatings systems (TBCs) that will be an essential part of their application in advanced turbines. This paper details the oxidation behavior in which

* Present Address: Stevens Institute of Technology, Hoboken, New Jersey, USA.

one of the Ni-based single crystal superalloys, René N5 (General Electric Aircraft Engines) from the ATS single crystal casting program conducted by PCC Airfoils, Inc. [2], is used as the substrate. In addition, cast (not single crystal) γ -NiAl optimally-doped with Zr, which has been found to form an essentially 'ideal' alumina scale [21-23] was used as a model bond coat alloy.

EXPERIMENTAL PROCEDURES

A yttrium-doped single crystal superalloy, René N5, was used as a basis for comparison for desulphurised, Y-free versions of the same alloy (denoted as N5^{*}). Desulphurisation was performed by PCC Airfoils Inc. [2] using a proprietary in-melt technique, a post-solidification hydrogen treatment, and a combination of both. Alloy N5^{*}A is nominally René N5 without Y and not desulphurised; alloy N5^{*}AH was hydrogen-desulphurised; alloys N5^{*}B and N5^{*}C were melt-desulphurised; and alloy N5^{*}BH was melt-desulphurised and then hydrogen annealed. A Zr-doped NiAl alloy was produced by vacuum arc melting. The chemical compositions of the alloys are shown in Table I. The sulphur levels of the alloys subjected to desulphurisation were measured by the glow discharge mass spectroscopy technique (GDMS). At present there are uncertainties when using GDMS to measure very low levels of sulphur because of the lack of a sulphur standard in the appropriate range. Hence, the absolute values of the sulphur contents shown in Table I are questionable. Nevertheless, in the absence of more definitive sulphur measurements, the values reported from GDMS analyses are used in the paper. Overall, the compositions of René N5 and the Y-free derivatives were close to the nominal composition with the exceptions that the Y content of René N5 was half that expected, and the Ti contents of all the alloys were low. Note, also, that the alloys subjected to hydrogen annealing had been essentially decarburised.

Specimens of approximate dimensions 20 x 10 x 1 mm were cut by electrode discharge machining from specially cast single crystal bars, so that the large surfaces of the specimens corresponded to the same crystal orientations as the surfaces of an airfoil. The specimen surfaces were polished through 600 grit SiC papers prior to oxidation; specimens intended for detailed examination of the scales were polished through 0.3 μ m alumina prior to oxidation (the difference in surface finish was found to make a small difference in the initial weight gain, but no difference in the shape of the oxidation curve). All specimens were measured to 0.01 mm and weighed to 0.01 mg, then ultrasonically degreased in acetone and methanol before oxidation. Specimens were suspended in the oxidation furnaces from Pt-Rh wires. Appropriate corrections for evaporative loss of Pt and Rh were made in evaluating the oxidation kinetics.

The cyclic oxidation test cycle involved heating from near ambient temperature to test temperature, holding at temperature for 1 hr or 100 hr, before cooling. Tests with a 1-hr dwell time at temperature were conducted in an automatic rig in which individually suspended specimens were introduced directly into a hot furnace into which oxygen was slowly flowing. At the end of each exposure period, the specimens were withdrawn into individual ceramic housings for a 10-min. cooling period. This cycle was interrupted for weighing every 20 or 50 cycles. In a second cyclic oxidation test, individual specimens were placed in lidded, pre-annealed alumina crucibles and exposed in air in an electric box furnace. The specimens were loaded into the cold furnace, which was then heated and held at temperature for 100 hr, and then allowed to cool, after which the specimens were removed and weighed. By weighing each crucible with and without the specimen, the specimen weight change and the weight change due to the total uptake of oxygen were obtained. Isothermal oxidation kinetics also were measured for direct comparison. These exposures were carried out in dried oxygen in a Cahn model 1000 microbalance, which weighed to 0.01 mg. The runs were started by lowering specimens into a heated furnace; at the end of the exposure period, they were quickly removed from the furnace.

The test temperatures ranged from 1050 to 1200°C; the projected maximum temperature experienced by the bond coating-ceramic interface of TBC-bearing airfoils in advanced land-

based gas turbines is at the low end of this range, whereas airfoils in aircraft gas turbines may experience peak metal temperatures at the higher end of this range.

After oxidation the specimens were examined in a low-power stereo optical microscope. Selected specimens were mounted, cross sectioned and metallographically polished for examination by conventional light microscopy, while others were prepared for examination in a scanning electron microscope equipped with a field-emission gun (FEG) and energy-dispersive X-ray spectroscopy (SEM/EDS). Concentration profiles across mounted and polished cross sections were measured using an electron probe microanalyser (EPMA) equipped with a wavelength dispersive spectroscope.

EXPERIMENTAL RESULTS

Isothermal Oxidation

René N5

A parabolic plot of the isothermal oxidation kinetics for René N5 in oxygen at 1100, 1150, and 1200°C, shown in Fig. 1a, indicates that the overall oxidation behavior of this alloy approximated a parabolic rate law over the 100 h exposures reported, even though the values of the rate law exponent (n) calculated from the data ranged from 1.9 to 3.6. These values are shown in Table II, which also lists derived parabolic rate constants (k_p). The scale thicknesses calculated from the microbalance data (assuming the scale to be all Al_2O_3) were 0.9, 1.4, and 4.1 μm at 1100, 1150, and 1200°C, respectively, which corresponded well with measurements from cross sections.

René N5 formed a grey-appearing, adherent Al_2O_3 scale which, with increasing time and increasing temperature, developed a blue cast which was associated with an outer layer of Ni,Al-based spinel. The surfaces also contained small (approximately 150-200 μm in diameter) blue-appearing areas of localised spallation which increased in number with time and temperature. These areas are shown in low-magnification topographical views of the scale after 100 h at 1150 and 1200°C in Figs. 1b and 1c, respectively, and were associated with 2 to 10 μm -sized Ta-rich phases in the alloy surface. These blue-appearing areas did not appear to be present in the initial scale, but developed with time. Fig. 2a indicates that such Ta-rich particles that intersected the alloy surface were undercut by the growing alumina scale, and effectively isolated from the alloy. At some point, the scale surrounding them fractured and spalled, typically at or near the metal-oxide interface (Fig. 2c). For the isothermally-exposed specimens, this event probably occurred on cooling from the test temperature at the end of the test since the bare alloy surface was visible in plan views (Fig. 2b). On specimens exposed in the cyclic tests these areas were overgrown with voluminous scales of mixed oxides.

The main protective scales are shown in plan in Figs. 3a and b and in cross section in Figs. 3c-f. Small (approximately 0.1 μm -sized) Ta precipitates were found in the grain boundaries of the adherent alumina scale, and as small particles in the transient, outer scale, as is evident in cross sections after 100 hr at 1150 and 1200°C (Fig 3c, d). Ta incorporated into the alumina scale would be expected to migrate to the outer surface of the scale [20,24], so that it is not clear if the Ta particles on the outer surface of the scale were part of the initially-formed transient scale, or developed with time. The bulk of the relatively thick, outer layer of presumed transient scale was a Ni,Al spinel. Fracture cross sections (Fig. 3e,f) showed the structure of the main alumina scale to be mostly columnar, but the structure was not as consistently columnar as, for instance, on an ideally-doped NiAl alloy [22].

Y-Free and Desulphurised Alloys

The isothermal oxidation kinetics of the Y-free variants of René N5 with different degrees of desulphurisation are shown as parabolic plots in Fig. 4, and the calculated rate law exponents and derived parabolic rate constants are shown in Table II. In general, the isothermal oxidation behavior of the N5 alloys was little different from that of René N5. The rate constants in Table II suggest that the oxidation rate of René N5 was slightly slower than the Y-free alloys at all three temperatures, but any such trend was small.

The scale formed on alloy N5A spalled extensively on cooling from the test temperatures. The appearance of the scales of the other N5 alloys was similar to that of those formed on René N5: they were essentially grey with a few blue spots, and developed an increasingly blue cast and more numerous blue spots with increasing temperature. The surfaces of the scales formed on N5AH after 100 hr at 1150°C, and on N5BH after 100 hr at 1200°C are shown in Figs. 5a and b, and 6 a and b, respectively. On N5AH, the circular (blue) areas did not exhibit spallation to the alloy surface, and in the vicinity of these areas were faceted crystals of NiO (Fig. 5b), and bright-appearing Ta-rich particles were evident on the surface of the alumina scale. Figure 6a indicates spallation to the alloy at some of the circular areas and along the edge of the specimen of N5BH oxidised for 100 hr at 1200°C. Areas of general spallation on this surface exhibited large crystals of Ni,Al spinel (shown in Fig. 6b). Bright-appearing Ta-rich particles also were visible on the surface of this scale.

Fracture cross sections of these scales, shown in Figs. 5c and 6c, indicated that the main alumina scale on both alloys had a columnar structure that was as well developed as that on René N5, despite there being no Y dopant present. This structure is indicative of doping of the scales with a reactive element; in these cases the dopant is presumably Hf (Table I), although the transmission electron microscopy of these scales required to confirm this assumption has not yet been completed. The thicknesses of the alumina scales corresponded well with those calculated from the overall weight gains.

Cyclic Oxidation

René N5 and Desulphurised Variants

Cyclic oxidation kinetics (1-hr cycles) of the alloys at 1100 and 1150°C are shown in Figs. 7a and b. While an improvement in resistance to scale spallation is obvious from the data for 1100°C when the sulphur level was reduced from 5-6 ppma (N5A) to approximately 0.8 ppma (N5C) in the absence of Y-doping, there was not much discrimination among the kinetics of alloys with lower sulphur levels, nor between René N5 and the lower sulphur alloys at this temperature. It was assumed that the maximum in the specimen weight gain curve could be used to indicate the time at which major spallation of the scale started, and the isothermal kinetic data were used to estimate the oxide thickness at that time. For N5A, the estimated maximum scale thickness attained before spallation initiated was relatively small, approximately 0.9 µm. The scale thicknesses on the other alloys which did not exhibit major spallation ranged up to approximately 2.2µm.

At 1150°C, alloys N5B and N5C (1.5 ppma S and 0.8 ppma S, respectively) suffered weight losses due to scale spallation at earlier times than René N5 and alloys N5AH (1.3 ppma S) and N5BH (0.6 ppma S). Cyclic oxidation results from other work in this study indicated a consistent improvement in scale spallation behavior for alloys N5AH, N5BH, and N5C, but that the order of improvement was N5BH>N5AH>N5C, possibly suggesting that the sulphur levels of the first two alloys are lower than for N5C, contrary to the chemical analysis results. The estimated scale thicknesses at which major spallation started at 1150°C was 1.0 to 1.2 µm for N5B and C, and 1.9 µm for René N5. Alloys N5AH and BH attained estimated scale thicknesses of 4.9 to 5.5 µm without apparent spallation. Figs. 8a and b present a comparison of the cyclic and isothermal kinetics for René N5, N5A and N5C at 1100 and 1150°C, respectively. Assuming that the difference between the isothermal and cyclic kinetic curves is a measure of scale loss by spallation in the cyclic test, the degree of spallation appears to decrease with decreasing S levels, and to increase with increasing temperature. The spallation observed from René N5 apparently was a reflection of the fraction of the oxide surface affected by Ta-rich particles.

The kinetics from the test involving 100-hr. cycles at 1100°C are shown in Fig. 9. These data also indicate a trend to decreased scale spallation with decreased alloy sulphur level. Compared to the 1-hour cyclic test at 1100°C, this test provided more discrimination among the alloys, with results similar to the 1-hour cycle test at 1150°C. The fact that the N5BH alloy (0.6 ppma S) exhibited early spallation was unexpected; the estimated scale thickness at which this started was 2.4 µm. The scale thicknesses corresponding to the onset of spallation on N5A, N5B, and N5C were 0.6, 1.5, and 3.0 µm, respectively, whereas René N5 and N5AH attained

estimated thicknesses of 4.7 to 5.0 μm without obvious spallation. The experimental procedures used in the 100-h cyclic test allowed a comparison to be made of the weight change of the specimen with the overall weight change due to oxygen pickup. As shown in Fig. 10, such comparisons for René N5 and N5AH indicate some degree of scale spallation from René N5, but very little spallation from N5AH. However, because the total weight gains of the two alloys were very similar, this may reflect spallation associated with Ta-rich particles (Fig. 2) and not a general spallation of the alumina scale.

Low-sulphur bond coating

A laboratory chemical vapor deposition (CVD) rig was modified to produce low-sulphur NiAl bond coatings on the desulphurised N5C [0.8 ppma S] substrate [25]. EPMA concentration profiles through the approximately 25 μm coating thickness (Fig. 11a) indicated relatively uniform levels of Ni and Al (approximately Ni_{1.3}Al), as well as Co (approximately 9 wt %) and Cr (approximately 3 wt %). There were also indications that heavy elements such as Ta, W, and Re had diffused into the aluminide coating, to levels of less than 1 wt %. In backscattered electron images the coating grain boundaries appeared much lighter than the adjacent grains, implying that these heavy element dopants were most likely segregated at the metal grain boundaries. Incorporation of sulphur into the coating was examined by GDMS, using sputtering on a flat surface of a coated specimen. Despite problems in interpreting the concentration profiles due to variations in sputtering rate within the sampled area, profiles for the major elements were consistent with the EPMA data. The sulphur level of the coating shown in Fig. 11b was approximately 11 ppmw at the beginning of sputtering, falling into the 1 to 2 ppmw range after 10 min. of sputtering, and then rising to approximately 7.5 ppmw after 150 to 170 min. of sputtering. The concentration profiles for sulphur and oxygen made by the same technique in the uncoated N5C substrate remained relatively flat, with the indicated sulphur level in the range 0.3 to 0.5 ppmw (0.6 to 0.9 ppma), Fig. 11c.

The sulphur peak on the coating surface was found to result from the coating process (from Viton 'O'-rings). This outer S-rich layer was removed before oxidation exposures by mechanically polishing the coating surface [25]. The inner sulphur peak appeared to be located in the same region as the refractory element-rich 'diffusion region' between the coating and the substrate. As shown in Fig. 12a, the scale spallation behavior of such a coating up to approximately 500 hours of thermal cycling in the 1-hr cycle test at 1100°C was essentially the same as for the uncoated N5C substrate, and was significantly improved compared to the undoped, non-desulphurised alloy (N5A). When scale spallation occurred from the coating after 500 cycles, the loss of scale was from the vicinities of the surface grain boundaries of the coating; an adherent alumina scale continued to form over the grain bodies of this coating. Elements such as Ta, Co, Cr, and W from the superalloy substrate were found to be enriched in the coating grain boundaries, and led to the formation of less protective, less adherent oxides over these regions. Figures 12b and c illustrate the surface topography of the coating before and after oxidation, and show the nature of the scale spallation. The formation of grain boundaries in these coatings appeared to be associated with impurities such as oxide particles present on the substrate surface prior to coating.

TBCs on N5 Substrates

Figure 13a shows the oxidation kinetics from a 1-hour cycle test at 1150°C for René N5, N5A and N5C coated (on all sides) with a state-of-the-art platinum-aluminide bond coating, and on one side with a top coat of yttria-stabilised zirconia (YSZ) deposited by electron beam physical vapor deposition (EB-PVD). The criterion used to assess failure of the TBCs was the loss of at least 20 percent of the ceramic layer on the flat surfaces of the specimens. The loss of small chips of ceramic from the edges of the specimens was discounted, since the specimen shape and dimensions were not optimised to accommodate a TBC. The ceramic layer on N5A failed after 300 cycles; on N5C failure occurred after 450-500 cycles; whereas the TBC on René N5 failed after 650 cycles. On this basis, the life of the coating on the non-desulphurised, Y-free substrate (N5A) was approximately one half that on René N5, whereas the life of that on N5C (0.8 ppma S) was approximately 75 percent that on the Y-containing alloy.

TBCs on an 'ideal' alumina-forming bond coating

The same EB-PVD YSZ coating was directly applied to one side of specimens of the model bond coat alloy γ -NiAl-Zr to demonstrate the potential spallation-free lifetime possible when the bond coating forms an ‘ideal’ alumina scale [23]. Previous studies [21,22] have shown that this alloy forms an γ -Al₂O₃ scale that grows almost entirely by oxygen transport, at a rate up to 2 to 4 times slower than that formed on undoped NiAl (or other undoped alumina-forming alloys), and which shows only edge spallation at temperatures in the range studied here for times in excess of 2,500 hours (oxide thickness greater than 9 μ m). As shown in Fig 13b, the lifetime of the ceramic layer on this substrate was more than 2,500 cycles, at least four times that of the René N5-PtAl bond coat system in the same test. Surprisingly, a YSZ coating deposited by plasma-spraying directly onto the polished surface (600 grit finish) of the γ -NiAl-Zr alloy was found to spall only after 1,200 cycles, which was almost double the lifetime of the René N5-PtAl-EB-PVD YSZ system in the same test [23].

DISCUSSION AND CONCLUSIONS

Desulphurisation of Y-free René N5 using a production-scale process was found to be capable of achieving excellent resistance to scale spallation, at least under the conditions of the tests used in this study. Overall, there appeared to be little obvious difference in the performance of René N5, and a Y-free version desulphurised by post-solidification hydrogen annealing to an indicated sulphur level of 1.3 ppma (< 0.05 ppma C), or by a combination of in-melt processing and post-solidification hydrogen annealing to a sulphur level of 0.6 ppma (< 0.05 ppma C). In 1-hr cycle tests at 1100°C, desulphurisation to the order of 1.5 ppma appeared sufficient whereas, in 100-hr cycle tests at 1100°C and 1-hr cycle tests at 1150°C, improved scale spallation resistance was not experienced until lower sulphur levels were achieved. Given the uncertainty of the absolute value of the final sulphur level of the desulphurised alloys, it appeared that the one of the best-performing alloys (N5^{BH}, 0.6 ppma S) probably was desulphurised to a sulphur level near that found to be optimum by Smialek [13], and which corresponded to a surface coverage of sulphur upon segregation of less than one monolayer. The other best-performing alloy (N5^{AH}) had apparently been desulphurised to only 1.3 ppma.

The composition of René N5 includes small additions of Hf, Zr, and Ti (Zr is not a specified addition, but probably is present as an impurity with Hf) in addition to Y, all of which are elements that have been considered to exert a ‘reactive element effect’ during high-temperature oxidation. If indeed a major manifestation of the reactive element effect is to prevent or inhibit the segregation of tramp sulphur at the substrate-oxide interface, it is of interest to enquire why, in the absence of Y, Hf or Zr did not exert any beneficial effect in alloy N5^A. There is significantly more Hf present in the alloy than there is Y, and Hf as well as Y was found to be segregated to the grain boundaries (and presumably the scale-substrate interface) of the protective oxide [23]. One factor may be that, while both Y and Hf form extremely stable oxides (with Y₂O₃ being the more stable—having a more negative free energy of formation—than HfO₂), Y also forms very stable sulfides (Y₂S₃, and YS), whereas the stability of Hf sulfide (HfS₂) is significantly lower, of the same order as the most stable sulfides of Ti and Zr [26]. Also, while both Y and Hf form very stable carbides and nitrides, in both cases the Hf compounds (HfC and HfN) have a significantly more negative free energy of formation than the Y compounds (YC₂ and YN). As pointed out by Sigler [26], these differences suggest that Hf most likely would react with carbon, nitrogen and possible oxygen before completely reacting with sulphur. In contrast, while Y will react strongly with oxygen and sulphur, it is likely to react preferentially with sulphur because of the much greater differential in free energy of formation between Y₂S₃ and Al₂S₃ than between Y₂O₃ and Al₂O₃.

The two Y-free, desulphurised alloys that exhibited the most improved resistance to scale spallation (N5^{AH} and BH) also had been decarburised as a result of the hydrogen annealing part of the desulphurisation process (see Table I). Although analysis is not presently available, it is possible that decarburisation influenced the improvement in resistance to scale spallation by, for instance, allowing the Hf content of the alloys to play a more active role (similar Hf contents in NiAl produce slow-growing, very adherent alumina scales). Further, the less detrimental role of Ta-rich particles on local scale spallation from these two alloys may also

have been a result of the removal of carbon allowing, for instance, more uniform distribution of Ta in the alloys.

The thermal cycle tests which used a 1-hr dwell time at temperature were very similar to those used as standard screening tests in the gas turbine industry, intended as a simplified simulation of the most severe part of the duty cycle experienced by aircraft engines. In fact, the duty cycle of advanced power generation turbines will probably consist of a relatively fast ramp up from cold to maximum power, followed by long periods at essentially maximum power, punctuated by short periods of operation at partial load. The 1-hr cyclic tests will not provide a representative simulation of this operation. Also, the maximum metal temperature experienced by the bond coating-ceramic interface is not expected to exceed approximately 1050°C, significantly lower than the peak temperatures of 1150 to 1175°C typically used in aircraft gas turbine simulation tests. From this perspective, comparison of the overall trends from the 1-hr and 100-hr cyclic tests at 1100°C reported here is pertinent. The observation that lower sulphur levels were required to resist scale spallation in the 100-hr cycle test indicates that this was, in fact, a more severe test than the 1-hr cycle test at the same temperature. Although the 1-hr cycle test results in more frequent exposure to stresses from differential thermal expansion between the alloy and the scale, the incremental increase in scale thickness between individual cycles is relatively small so that, possibly, the increase in stress is easier to accommodate without scale buckling or cracking than with the thicker scale formed after a 100-hr cycle. The longer cycle time may also allow time for the growth of interfacial voids, which may contribute to the increased spallation.

The initial results shown here for NiAl coatings suggest that desulphurisation of coatings is probably achievable in the relatively near-term. The growth of less protective scale associated with oxidation of elements diffusing from the superalloy substrate along the grain boundaries of such coatings remains a problem. However, the observation that grain boundaries in these coatings appear to grow from impurities in the original substrate surface suggests that the number of grain boundaries could be reduced by relatively straightforward modification of the coating process, which could lead to a further improvement in resistance to scale spallation. Nevertheless, the added benefit of reactive element doping to give reduced scale growth rates remains a desirable goal, since any alumina scale eventually will be prone to spallation when it attains some critical thickness at which the stresses from continued growth and the imposed stresses from thermal cycling and thermal expansion mismatch with the substrate and external YSZ layer cannot be accommodated without buckling or cracking.

The state-of-the-art Pt aluminide bond coating used in the TBC applied to specimens of René N5 typically forms an alumina scale that is very resistant to spallation. In the 1150°C/1-hr cycle test, the observed increase in life with decreasing sulphur level in the substrate of the TBC based on this bond coating suggests that sulphur from the substrate can decrease the resistance to spallation of the scale formed on the Pt aluminide. This is surprising since, as detailed elsewhere [27], undoped Ni,Pt-Al (50 at% Al) alloys with sulphur levels of approximately 20 ppm formed alumina scales which were extremely resistant to spallation in this test at scale thicknesses greater than 4 µm.

The effectiveness of the optimally-doped -NiAl-Zr alloy (compared to the undoped Pt-aluminide layer on the Y-doped superalloy) in retaining an external YSZ layer in the thermal cycling tests resulted from four main factors. The first two factors were the reduced rate of growth of the oxide and the lack of void formation at the substrate-oxide interface, both of which are manifestations of the reactive element doping in this alloy. The third and fourth factors resulted from the fact that a monolithic alloy was used as the 'bond coating.' Hence, there were no unwanted elements able to transport to the oxidising surface and become incorporated into the scale, and that there was always sufficient aluminum available for protective scale formation since there was no loss by interdiffusion with a substrate. These advantages are obviously difficult to realise in a practical coating. A further difficulty is in controlling the dopant level and its uniform distribution in a practical coating process, especially since over- and under-doping may be detrimental to performance [22].

ACKNOWLEDGMENTS

This research was supported in part by the U.S. Department of Energy Office of Industrial Technologies as part of the Advanced Turbine Systems Program, and in part by the Division of Materials Sciences under contract DE-AC05-96OR22464 with Lockheed Martin Energy Research Corporation. We would like to thank Dr. B. Nagaraj of the General Electric Aircraft Engines Group for supplying samples of René N5 and the EB-PVD TBCs; Dr. W. Brindley of NASA-Lewis Research Center for applying the plasma sprayed ceramic coating; and Dr. C. T. Kortovich of PCC Airfoils, Inc., who supplied the desulphurised alloys. We would also like to thank colleagues at ORNL and in the aerospace alloy casting and coating supply industry for their useful comments and discussion throughout the course of this work.

REFERENCES

1. 'Materials/Manufacturing Plan for Advanced Turbine Systems Program,' Office of Industrial Technologies, Rpt. No. DOE/OR-2007, April 1994.
2. C. S. Kortovich, R. M. Garlock, and C. R. Hayes: 'Turbine Airfoil Manufacturing Technology,' Paper No. 97-GT-428, presented at the 42nd ASME Gas Turbine and Aeroengine Congress, Exposition, and Users Forum, Orlando, Florida, June 1997.
3. B. A. Mueller, A. R. Price, K. S. Murphy, and G. B. Bell: 'Land-Based Turbine Casting Initiative,' paper No. 97-GT-430, presented at the 42nd ASME Gas Turbine and Aeroengine Congress, Exposition, and Users Forum, Orlando, Florida, June 1997.
4. N. S. Bornstein and J. Marcin: 'Pratt and Whitney Thermal Barrier Coatings,' pp. 182-193 in Proc. Advanced Turbine Systems Annual Program Review Meeting, C. T. Alsup, C. M. Zeh, and S. Blazewicz, eds., DOE/METC-96/1023, Vol. 1 (DE96000561), 1996.
5. J. Goedjen, S. Sabol, and G. Wagner: 'Westinghouse ATS Thermal Barrier Coatings Development,' Proc. Advanced Turbine Systems Materials Workshop, Charleston, SC., Feb 13-14 1996.
6. Y. Ikeda, K. Nii, and K. Yoshihara: 'High-temperature oxidation and surface segregation of sulphur,' pp. 207-214 in Proc. JIMIS-3: High-Temperature Corrosion Transactions of the Japan Inst. of Metals, Supplement 24, 1983.
7. A. W. Funkenbusch, J. G. Smeggil, and N. S. Bornstein, *Met. Trans.*, 1985, **16A**, 1164.
8. J. G. Smeggil, A. W. Funkenbusch, and N. S. Bornstein, *High-Temp. Sci.*, 1985, **20**, 163.
9. J. G. Smeggil, A. W. Funkenbusch, and N. S. Bornstein: 'A relationship between indigenous impurity elements and protective oxide scale adherence characteristics,' *Met. Trans.*, 1986, **17A**, 923.
10. K. L. Luthra and C. L. Briant: 'Adhesion of oxide films on MCrAlY alloys,' pp. 187-199 in Fundamental Aspects of High-Temperature Corrosion-II, D. A. Shores, and G. R. Yurek, eds., The Electrochemical Soc., Pennington, NJ, 1986.
11. J. L. Smialek: 'Adherent Al₂O₃ scales produced on undoped NiCrAl alloys,' pp. 297-313 in Oxidation of Metals and Associated Mass Transport, M. A., S. J. Rothman, and W. E. King, eds., The Metallurgical Society of AIME, 1986.
12. J. L. Smialek: 'The effect of sulphur and zirconium co-doping on the oxidation of NiCrAl,' pp. 241-7 in High Temperature Materials Chemistry IV, Z. A. Munir, D. Cubicciotti and H. Tagawa, eds., Proc. Vol. 88-5, Electrochemical Society Inc., Pennington, NJ, 1988.
13. J. L. Smialek: 'Effect of sulphur removal on Al₂O₃ scale adhesion,' *Met. Trans.*, 1991, **22A**, 739-752.
14. J. L. Smialek, D. T. Jayne, J. C. Schaeffer, and W. H. Murphy,: 'Effects of hydrogen annealing, sulphur segregation, and diffusion on the cyclic oxidation resistance of superalloys; a review,' *Thin Solid Films*, 1994, **253**, 285-292.
15. J. L. Smialek, and B. K. Tubbs, 'Effect of sulphur removal on scale adhesion to PWA 1480,' *Met. Trans.*, 1995, **26A**, 427-435.
16. J. L. Smialek: 'Oxidation resistance and critical sulphur content of single crystal superalloys,' Paper No. 96-GT-519, presented at the 41st ASME Gas Turbine and Aeroengine Congress and Exhibition, Birmingham, England, June 1996.

17. J. C. Schaeffer, W. H. Murphy, and J. L. Smialek: 'The effect of surface condition and sulphur on the environmental resistance of airfoils,' *Oxid. Met.*, 1995, **43** (1/2), 1-23.
18. G. H. Meier, F. S. Pettit, and J. L. Smialek: 'The effects of reactive element additions and sulphur removal on the adherence of alumina to Ni- and Fe-base alloys,' *Materials and Corrosion*, 1995, **46**, 232-240.
19. E. Schumann, J. C. Yang, and M. J. Graham,: 'Direct observation of the interaction of yttrium and sulphur in oxidised NiAl,' *Scripta Met.*, 1996, **34** (9), 136-1370.
20. B. A. Pint: 'Experimental observations in support of the dynamic segregation theory to explain the reactive element effect,' *Oxid. Met.*, 1996, **45**, 1-37.
21. B. A. Pint, J. R. Martin and L. W. Hobbs: '¹⁸O/SIMS characterisation of the growth mechanism of doped and undoped γ -Al₂O₃,' *Oxid. Met.*, 1993, **39**, 167-95.
22. B. A. Pint: 'The oxidation behavior of oxide-dispersed γ -NiAl: I. Short-term performance at 1200°C,' *Oxid. Met.*, 1998, in press.
23. B. A. Pint, I. G. Wright, W. Y. Lee, Y. Zhang, K. Prützner and K. B. Alexander: 'Substrate and bond coat compositions: factors affecting alumina scale adhesion,' *Mat. Sci. and Eng.*, 1998, in press.
24. B. A. Pint, A. J. Garratt-Reed and L. W. Hobbs: 'A possible role of the oxygen potential gradient in enhancing diffusion of foreign ions on γ -Al₂O₃ grain boundaries,' *J. Amer. Cer. Soc.*, 1997, in press.
25. W. Y. Lee, Y. Zhang, I. G. Wright, B. A. Pint, and P. K. Liaw: 'Effects of Sulphur Impurity on the Scale Adhesion Behavior of a Desulphurised Ni-Based Superalloy Aluminised by Chemical Vapor Deposition,' 1997, submitted to xxx.
26. D. R. Sigler: 'Aluminum oxide adherence on Fe-Cr-Al alloys modified with group IIIB, IVB, VB and VIB elements,' *Oxid. Met.*, 1989, **32**, 337-55.
27. E. C. Dickey, B. A. Pint, K. B. Alexander, and I. G. Wright: 'The effect of platinum on the growth and adhesion of γ -Al₂O₃ scales,' paper presented at The Inst. of Materials' 6th Intl. Conf. on Engineering the Surface: High-Temperature Surface Engineering, Edinburgh, Sept 1997.

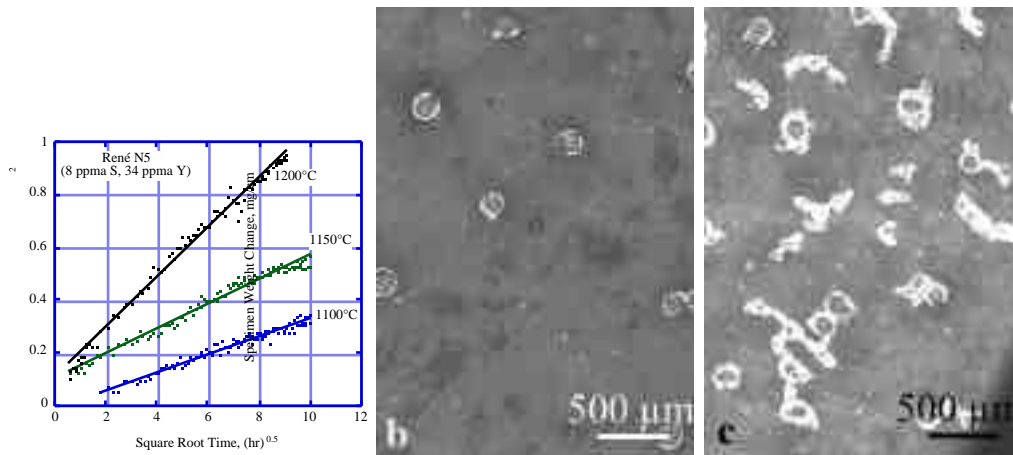


Fig. 1. Isothermal oxidation kinetics parabolic plot) of René 5 (a), and topographies of scale formed at (b) 1150°C and (c) 1200°C.

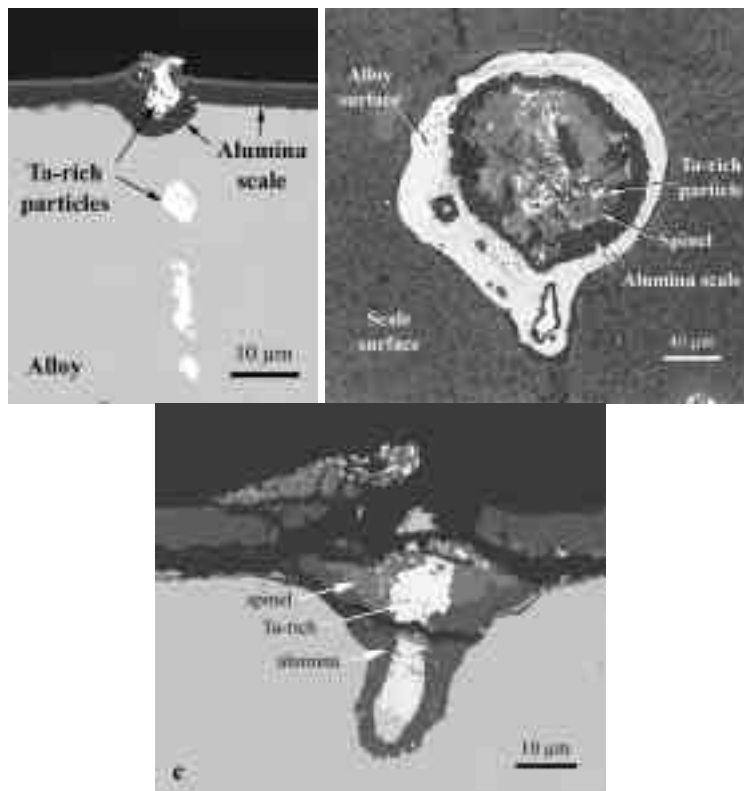


Fig. 2. Scale morphologies associated with local spallation on René N5 after isothermal oxidation at 1150°C for 100 hr showing (a) cross section showing incorporation of Ta-rich alloy phase into the scale; (b) topography of an area where spallation has occurred to the metal surface; and (c) a cross section of an area similar to (b) after 100 hr at 1200°C.

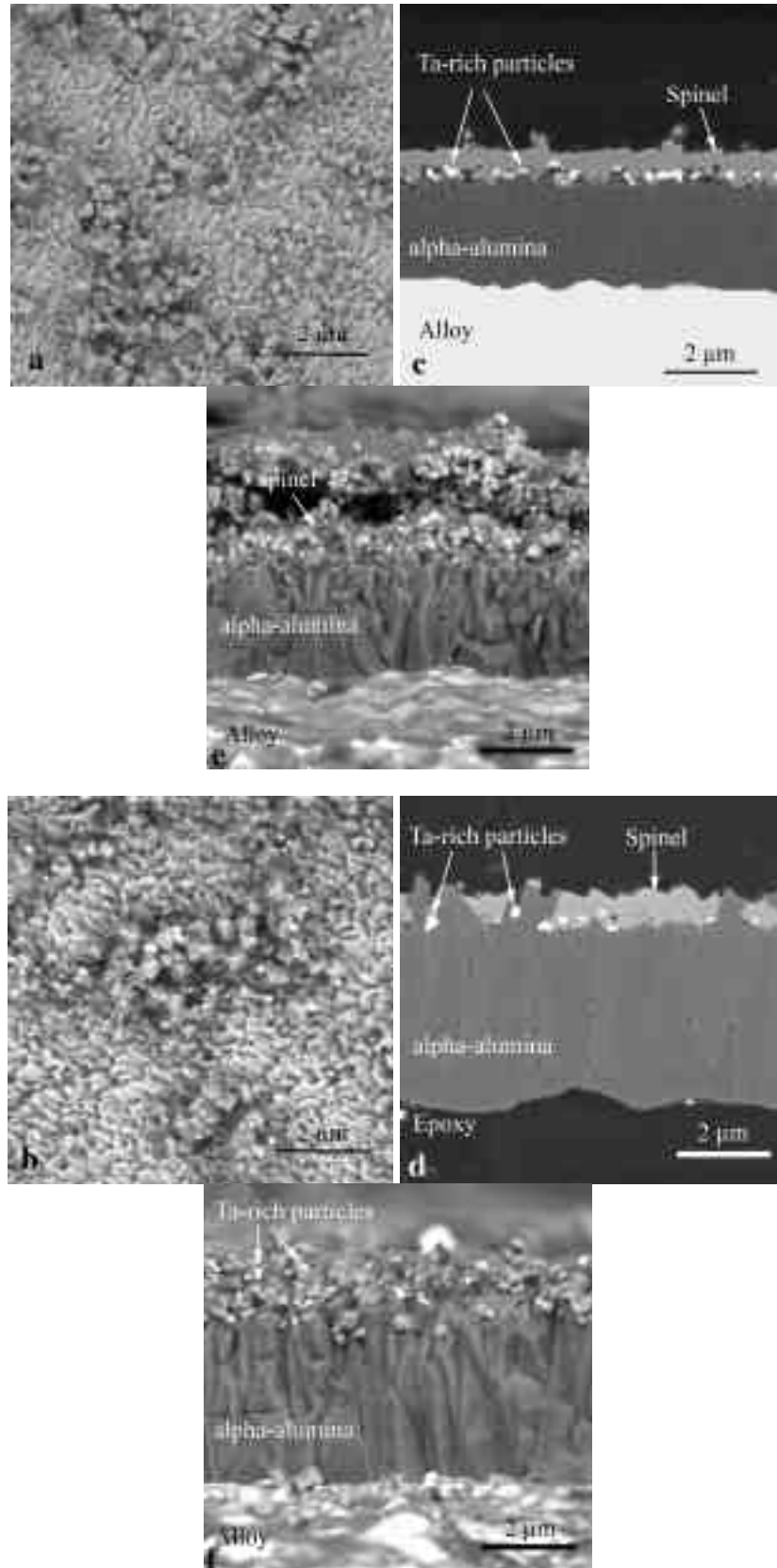


Fig. 3. Morphology of scale formed on René N5 after isothermal oxidation for 100 h at 1150 and 1200°C: (a) and (b) plan views; (c) and (d) SEM of cross sections; and (e) and (f) fracture sections of the scales.

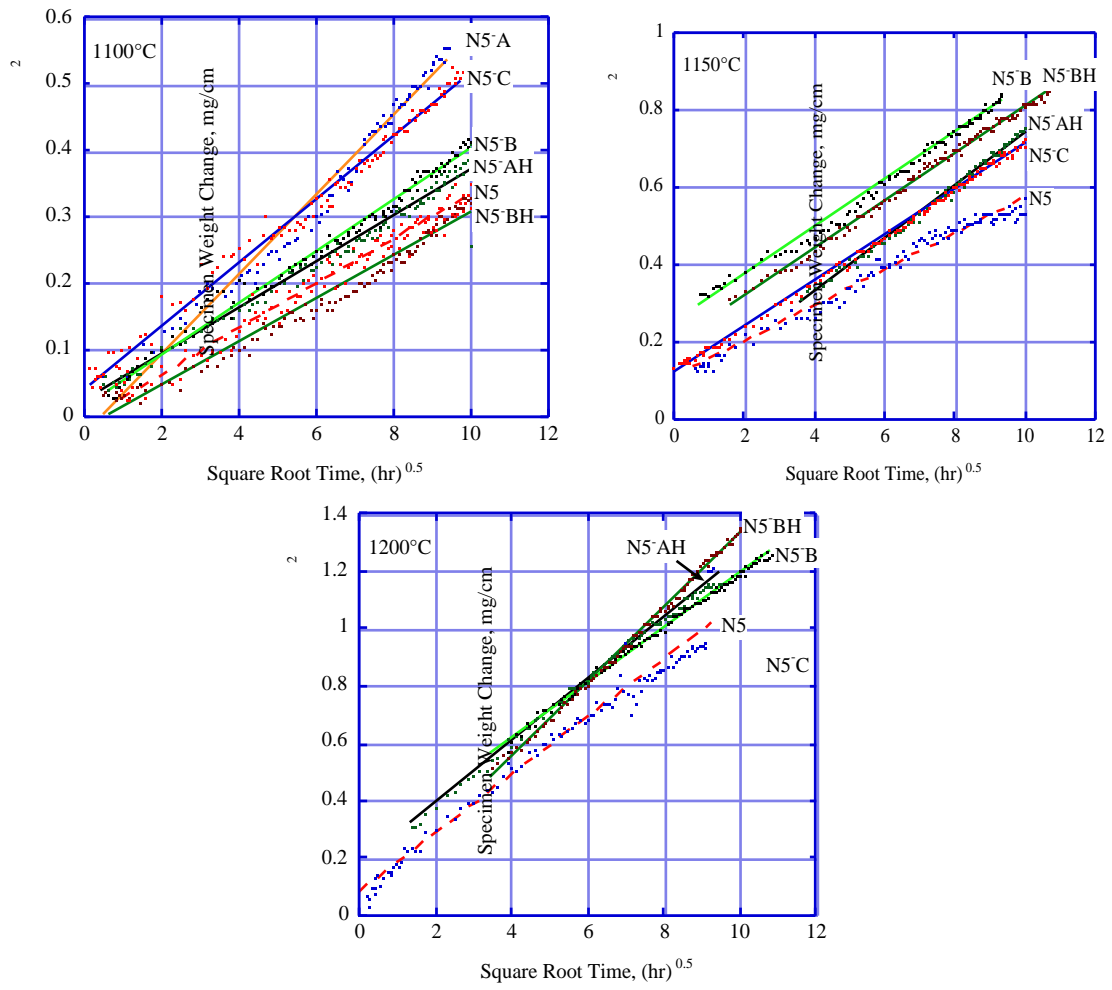


Fig. 4. Isothermal oxidation kinetics of desulphurised N5 alloys, parabolic plots.

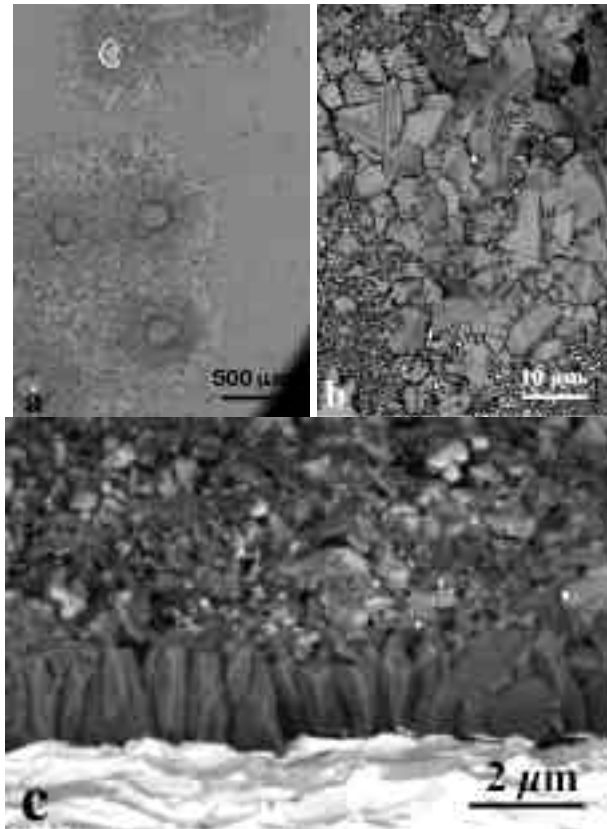


Fig. 5. Morphology of scale formed on N5-AH after isothermal oxidation for 100 h at 1150°C: (a) and (b) plan views; (c) SEM of fracture sections of the scale.

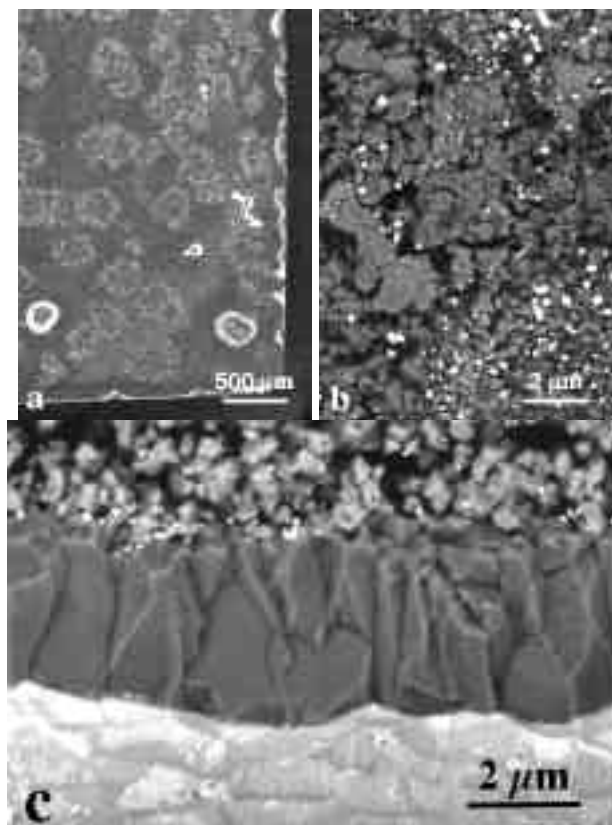


Fig. 6. Morphology of scale formed on N5-BH after isothermal oxidation for 100 h at 1200°C: (a) and (b) plan views; (c) SEM of fracture sections of the scale.

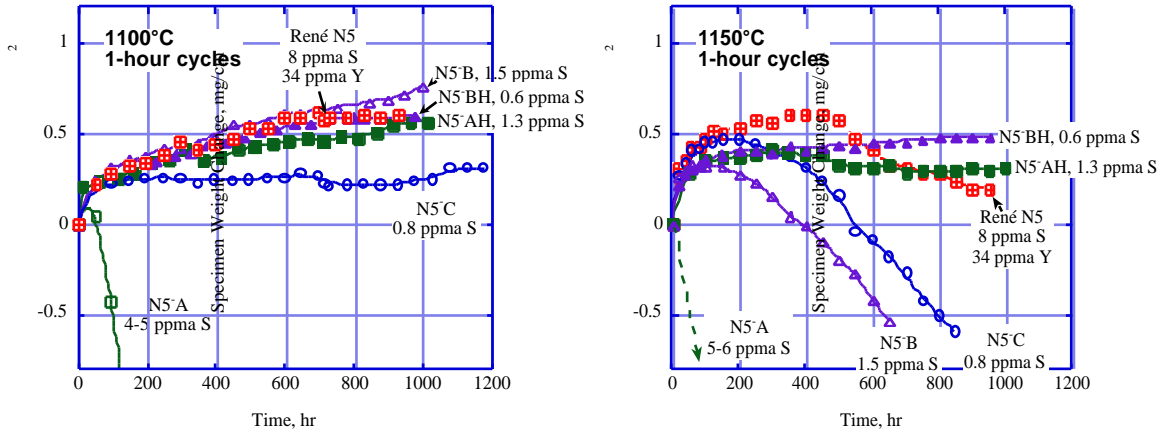


Fig. 7. Cyclic oxidation kinetics of desulphurised N5 alloys, 1-hour cycles

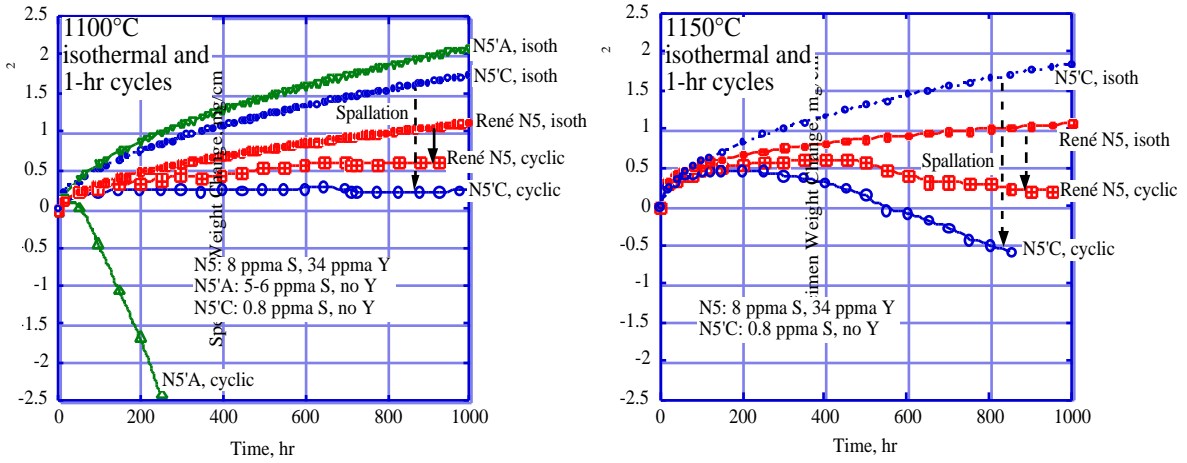


Fig. 8. Isothermal and cyclic (1-hr cycles) oxidation kinetics for René N5 and Y-free and desulphurised variants in oxygen at (a) 1100°C and (b) 1150°C.

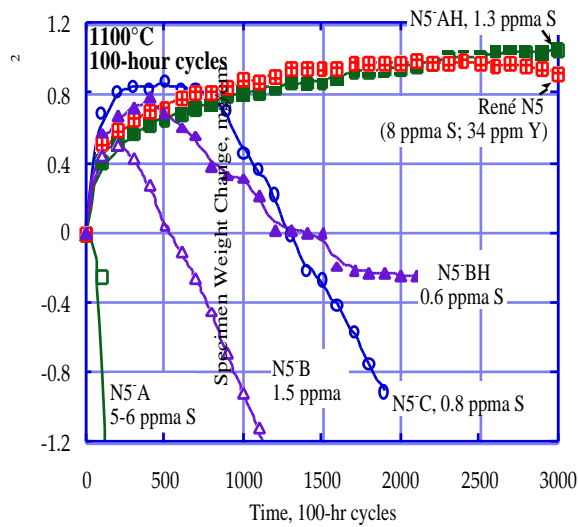


Fig. 9. Cyclic oxidation kinetics (100-hr cycles) at 1100°C in air

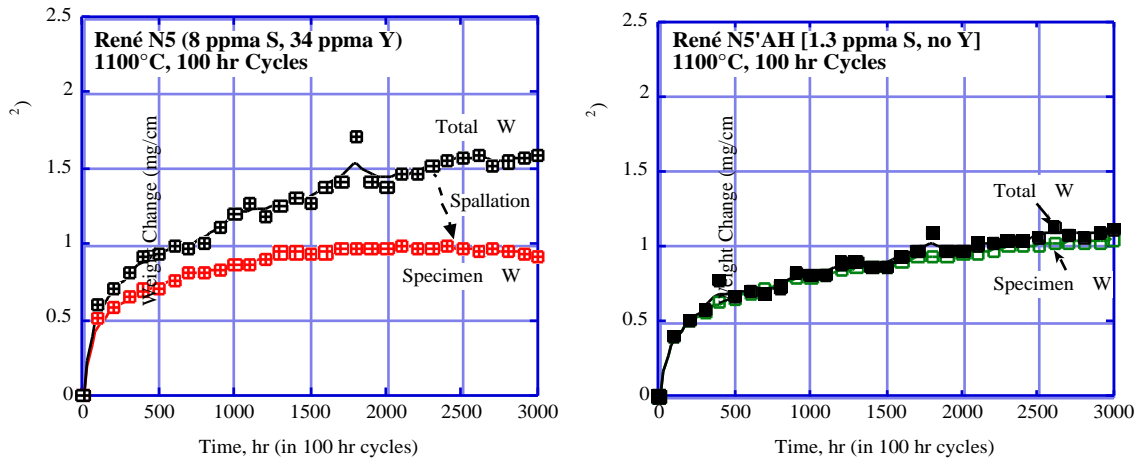


Fig. 10. Cyclic oxidation kinetics (100-hr cycles) at 1100°C in air showing the difference between the specimen weight change and the weight change due to the total oxygen uptake for (a) René N5 and (b) a Y-free variant (N5 AH) desulphurised to 1.3 ppm.

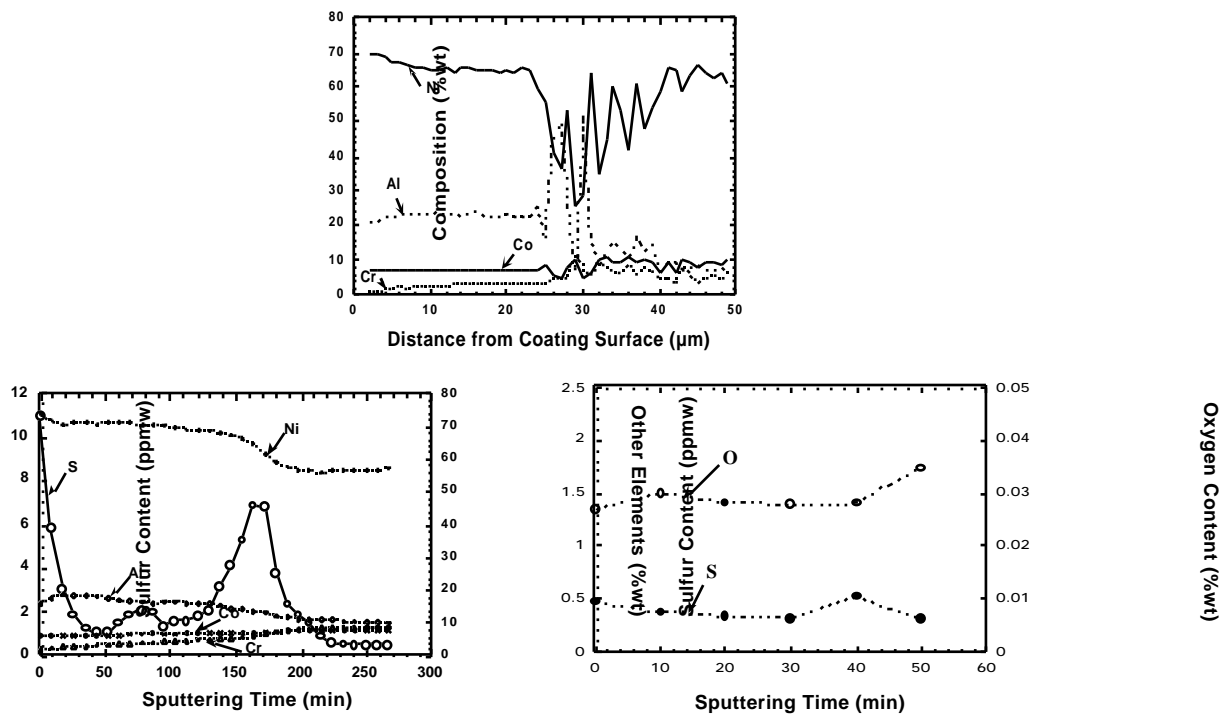


Fig. 11. Concentration profiles through the as-coated alloy by (a) EPMA; and (b) GDMS; and through the uncoated substrate by GDMS (c),

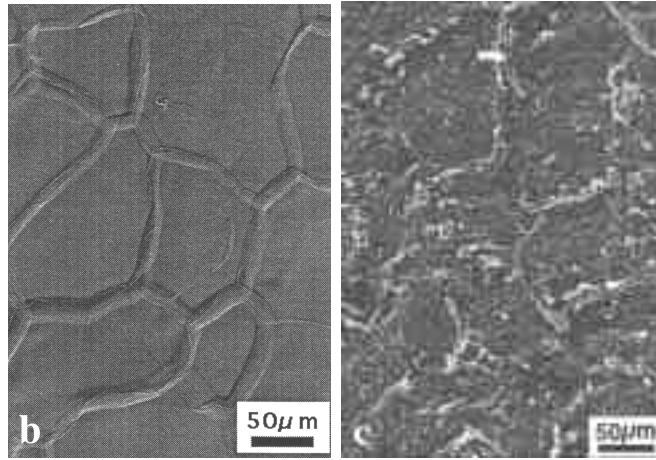
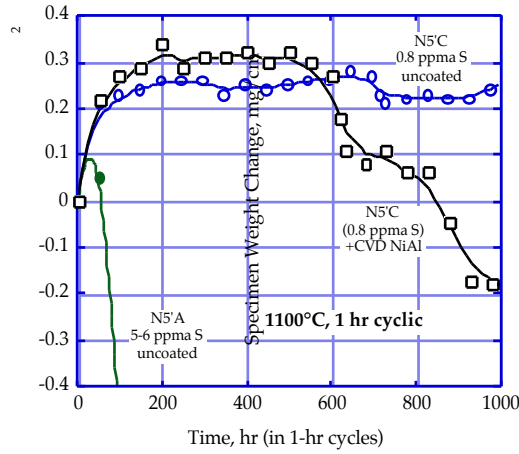


Fig. 12. Cyclic oxidation behavior (1-hr cycles, 1100°C) of Y-free, desulphurised (0.7 ppm S) René N5 with and without a low-S NiAl coating (a) kinetics (b) coating topography before exposure (c) coating topography after exposure

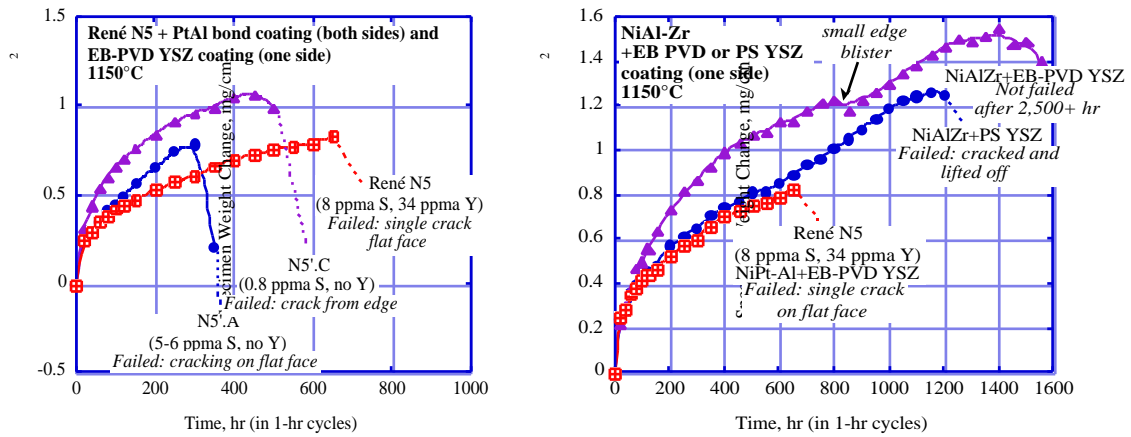


Fig. 13. Cyclic oxidation kinetics (1-hr cycles, 1150°C) of substrates with TBCs (a) René N5 and Y-free and desulphurised variants (b) René N5 compared to -NiAl-Zr.